

000 001 002 003 004 005 006 007 008 009 010 011 012 013 014 015 016 017 018 019 020 021 022 023 024 025 026 027 028 029 030 031 032 033 034 035 036 037 038 039 040 041 042 043 044 045 046 047 048 049 050 051 052 053 PAS: ESTIMATING THE TARGET ACCURACY BEFORE DOMAIN ADAPTATION

Anonymous authors

Paper under double-blind review

ABSTRACT

The goal of domain adaptation is to make predictions for unlabeled samples from a target domain with the help of labeled samples from a different but related source domain. The performance of domain adaptation methods is highly influenced by the choice of source domain and pre-trained feature extractor. However, the selection of source data and pre-trained model is not trivial due to the absence of a labeled validation set for the target domain and the large number of available pre-trained models. In this work, we propose **Potential Adaptability Score (PAS)**, a novel score designed to estimate the transferability of a source domain set and a pre-trained feature extractor to a target classification task before actually performing domain adaptation. **PAS** leverages the generalization power of pre-trained models and assesses source-target compatibility based on the pre-trained feature embeddings. We integrate **PAS** into a framework that indicates the most relevant pre-trained model and source domain among multiple candidates, thus improving target accuracy while reducing the computational overhead. Extensive experiments on image classification benchmarks demonstrate that **PAS** correlates strongly with actual target accuracy and consistently guides the selection of the best-performing pre-trained model and source domain for adaptation.

1 INTRODUCTION

In many real applications, data is collected from diverse domains, e.g., data obtained from different equipment, collecting procedures, geographic locations, or periods in time. Such differences may lead to a distribution shift between the domains that must be assessed. Unsupervised domain adaptation is a paradigm where only unlabeled data is available for the domain of interest, the target domain. However, labeled data is obtained from a related source domain.

One factor that affects the success of domain adaptation methods is the choice of the source domain data. Domain adaptation methods often rely on many assumptions about the relationship between source and target domains, like the existence of invariant discriminative features, the similarity of the label distribution, or the invariance of the task. Unfortunately, as the labels for the target samples are not available, such assumptions may not be verified in real applications for selecting the most appropriate source data. Violating the data assumptions and considering an irrelevant or distant source domain may introduce noise and conflicting patterns during the domain adaptation process. In the worst-case scenario, selecting an undesirable source domain may hurt the target domain performance, a scenario known as negative transfer Zhang et al.

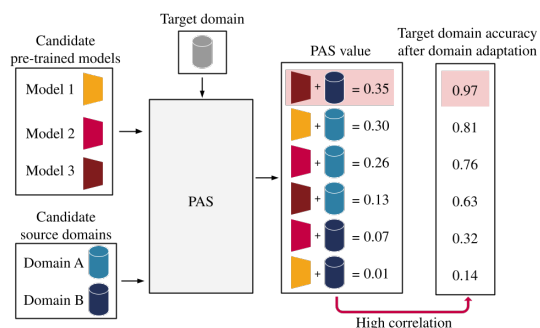


Figure 1: The **Potential Adaptability Score (PAS)** estimates the performance of adapting to an unlabeled target domain given a pre-trained feature extractor and a labeled source domain. It helps in the selection of the best pre-trained model and best source domain among many candidates and is highly correlated with the final target accuracy after domain adaptation.

(2022). If many source domains are available, it is reasonable to assume that not all of them may contribute equally to the target adaptation. Wisely selecting the source domain that may improve the performance on the target data while avoiding negative transfer is an essential requirement in many real-world applications.

Another key factor that influences the domain adaptation performance is the choice of the pre-trained model. Pre-training on large-scale data allows the models to learn generic features and patterns that are often transferable across domains and tasks, making them valuable for domain adaptation. Recently, practitioners can choose from a vast number of publicly available pre-trained models, spanning diverse architectures and training paradigms. Each pre-trained model may have its own inductive bias and may capture distinct patterns in the data that may be more or less useful when transferring knowledge between domains.

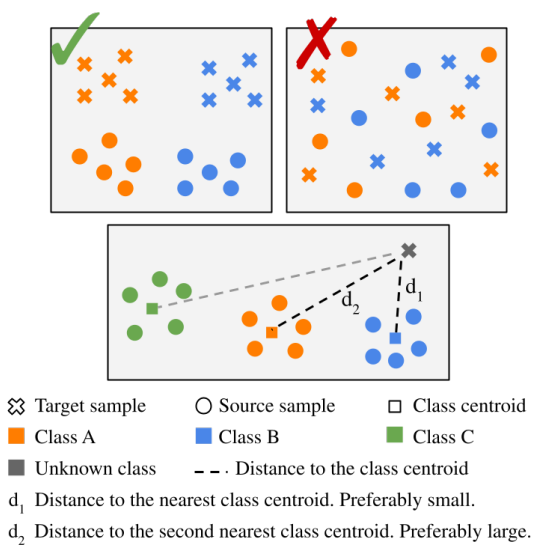


Figure 2: Source and target samples in the embedding space of a pre-trained model. (top left) Ideally, a target sample from a given class should be more similar, and hence closer in the embedding space of the pre-trained model, to a source sample from the same class. (top right) If new discriminative features need to be learned, the chances of overfitting on the source domain during adaptation increase. (bottom) Illustration of the distances from a target sample to all source class centroids. Our **PAS** score considers the relationship between distances d_1 and d_2 , which correspond to the shortest and second shortest distances, respectively.

challenging than transferring from the harder domain to the easier one.

In this work, we examine the interplay between the three key components in the domain adaptation setting for classification: (1) target data, (2) source data, and (3) the pre-trained model. We propose the **Potential Adaptability Score (PAS)**, a simple but effective novel measure to quantify the potential success of using a pre-trained model to transfer knowledge from a source domain to the target domain. Our experiments show how the **PAS** score is highly correlated to the final target accuracy after adaptation.

Despite the importance of selecting a suitable source data and a pre-trained model for the success of domain adaptation, it is still an underexplored topic. Current methods of transferability estimation aim to select the best pre-trained model for transfer learning. However, these methods are not applicable to the domain adaptation scenario since they require target labels Bao et al. (2019); Nguyen et al. (2020); You et al. (2021). One could employ such methods for selecting the best pre-training model using only the labeled source data and ignoring the unlabeled target data. Nevertheless, considering the target data is essential, as transferring to an easy target domain should lead to different results than transferring to a harder one.

Another approach for the problem would be performing domain adaptation for each combination of available source domains and pre-trained models, and applying some model selection strategy Ericsson et al. (2023); You et al. (2019). However, this approach is very time-consuming since it needs to run a domain adaptation algorithm for each combination.

A third approach would be to measure the distance between source and target feature distributions in the embedding space of the pre-trained model. This approach is also challenging as the popular metrics for the distance between two feature distributions are symmetric, e.g., Maximum Mean Discrepancy (MMD) Gretton et al. (2006), Wasserstein distance Vallet (1974), and CORAL Sun & Saenko (2016). However, a metric suitable for our scenario should be asymmetric because transferring from an easy to a hard domain is more

To the best of our knowledge, this is the first proposal for transferability estimation for the domain adaptation setting. We demonstrate how **PAS** can help to select the most relevant source domain and/or pre-trained model among a set of candidates, indicating the options that are most likely to lead to the best accuracy on the unlabeled target data (See an overview in figure 1.). Our framework selects the most suitable options before actually performing domain adaptation, demanding fewer computational resources and reducing the training time.

PAS leverages the generalization power of models pre-trained on a large-scale dataset, such as the popular ImageNet-1k Deng et al. (2009). Specifically for domain adaptation, initializing with a good pre-trained model appears to be a fundamental step in achieving a good transferability between domains Peng et al. (2018); Tang & Jia (2023); Kim et al. (2022); Li et al. (2023); Teterwak et al. (2023). We assume that a good pre-trained model can extract general discriminative features that are robust across all domains. If this assumption is true, samples from the same class are expected to be closer together in the embedding space generated by the pre-trained model, compared to samples from different classes, even in the presence of feature distribution shift. This ideal scenario is illustrated in the top left of the figure 2. Otherwise, as shown in the example on the top right of the figure, the model should learn new discriminative features during the adaptation from the limited labeled source data to enable the classification task, increasing the chances of overfitting to the source domain. Our **PAS** score is inspired by the Silhouette score, used for assessing the consistency of data clusters Rousseeuw (1987). We modify the original Silhouette score to measure the similarity of the unlabeled target samples to some of the known source class clusters defined in the pre-trained embedding space.

We summarize our contributions as follows:

- We propose **PAS**, a simple novel measure to quantify the potential contribution of a pre-trained model and labeled source domain in the adaptation to an unlabeled target domain before performing domain adaptation.
- We propose a framework to select the most relevant pre-trained model or source domain from a collection of potential candidates for performing domain adaptation.
- We empirically validate our framework using different domain adaptation methods and image classification benchmarks, and show how our score has a high correlation with the target accuracy.

2 RELATED WORK

Unsupervised domain adaptation. The goal of unsupervised domain adaptation (UDA) is to transfer the knowledge learned from a labeled domain to a different unlabeled target domain. Usually, this goal is achieved by learning a latent representation that is invariant across domains. Several works minimize the distribution discrepancy on the representation using statically defined distance metrics such as Maximum Mean Discrepancy (MMD) (e.g., DAN Long et al. (2015), DDC Tzeng et al. (2014), JAN Long et al. (2017)), covariance (e.g., DCORAL Sun & Saenko (2016)), or Wasserstein distance (e.g., DeepJDOT Damodaran et al. (2018)). The popularization of generative models inspired the proposal of methods that adopt adversarial learning to align data across different domains. DANN Ganin et al. (2016), CDAN Long et al. (2018), and ADDA Tzeng et al. (2017) are examples of widely adopted UDA methods that have shown promising results. Self-training is another promising paradigm that exploits the pseudo-labels predicted for the target domain to enhance the model. CST Liu et al. (2021), CRST Zou et al. (2019), FixMatch Sohn et al. (2020) and MCC Jin et al. (2020) are examples of methods that explore pseudo-labeling. Most recently, with the dissemination of transformers and foundation models, new works explore the cross-attention mechanism to propose transformer-based domain adaptation methods, such as PMTrans Zhu et al. (2023) and DoT Ren et al. (2024). See Liu et al. (2022); Deng & Jia (2023); Alijani et al. (2024) for a comprehensive survey on domain adaptation methods.

Pre-training and domain adaptation Recent works suggest that the choice of the pre-trained feature extractor can significantly improve the result of domain adaptation methods. Teterwak et al. (2023) show that simply adopting a model with better weight initialization can help the robustness of a model to out-of-distribution samples. Similarly, Kim et al. (2022) empirically show that SOTA pre-training outperforms SOTA domain adaptation methods even without access to a target domain.

With a modern pre-trained backbone, older domain adaptation methods perform better than SOTA methods, but no method is consistently better in all benchmarks, and negative transfer can occur. Li et al. (2023) empirically show how, in some cases, the performance of the pre-trained model in an unseen target domain is already decent. However, no single pre-trained model performs well in all target datasets. Tang & Jia (2023) study the effects of pre-training on the domain adaptation between synthetic and real images. Without pre-training, none of the methods considered in the study outperformed the baseline trained only on the labeled source data. Other studies have also proposed new datasets and pre-training techniques that achieve competitive performance in the target domain Shen et al. (2022); Luo et al. (2024). We leverage the potential relationship between pre-training and domain adaptation success to estimate transferability between domains.

Transferability estimation In the past years, many works have proposed scores for quantitatively estimating the transferability of a pre-trained model to a target task. One of the primary practical applications of such estimation is selecting the best pre-trained model for fine-tuning on the target data. H-score Bao et al. (2019), NCE Tran et al. (2019), LEEP Nguyen et al. (2020) and LogME You et al. (2021) are widely adopted transferability estimation scores. More closely related to our proposal, some works propose scores for transferability estimation by examining the separability of classes in the embedding space encoded by the pre-trained model. Pandy et al. (2022) apply the Bhattacharyya coefficient to quantify the target class separability. Similarly, Meiseles & Rokach (2020) employ the Silhouette score to assess the transferability of time series data. The current methods on transferability estimation focus on the transfer learning problem, where a pre-trained model is adapted to a target task with a few labeled samples. Unfortunately, these methods can not be applied to the domain adaptation problem, where the target labels are not available.

3 METHOD

3.1 DEFINITIONS

Unsupervised domain adaptation aims to transfer knowledge from a labeled source domain to an unlabeled target domain in the presence of distribution shift. Let $\mathcal{X} \subseteq \mathbb{R}^d$ define the input space and $\mathcal{Y} = \{1, \dots, C\}$ the label space. The labeled source dataset is denoted by $\mathcal{D}^S = \{(x_i^S, y_i^S)\}_{i=1}^{|\mathcal{D}^S|}$ and the unlabeled target dataset is denoted by $\mathcal{D}^T = \{x_i^T\}_{j=1}^{|\mathcal{D}^T|}$, with $x_i^S, x_i^T \in \mathcal{X}$ and $y_i^S \in \mathcal{Y}$. S_c^S denotes the set of source samples from class c . The source and target feature distributions are sampled from different but related distributions, $P_S(\mathcal{X})$ and $P_T(\mathcal{X})$, respectively, being $P_S \neq P_T$. This scenario is also known as *covariate shift*. The goal is to learn a hypothesis $h : \mathcal{X} \rightarrow \mathcal{Y}$ that performs well on the target domain.

Let θ be the parameters of a feature extractor $f_\theta : \mathcal{X} \rightarrow \mathcal{Z}$ pre-trained on a large-scale dataset. $z_i^S = f_\theta(x_i^S)$ and $z_i^T = f_\theta(x_i^T)$ denote, respectively, the embedding of a source and a target sample in the embedding space defined by f_θ .

3.2 ASSUMPTIONS

We assume that a good pre-trained model f_θ is able to extract a wide range of patterns and high-level concepts from an input, including discriminative features that are invariant across different domains. We expect that samples from the same class are more similar, having many concepts in common. As a result, two samples from the same class should be closer together in the embedding space \mathcal{Z} , no matter the domain. On the other hand, samples from different classes should have very few concepts in common, resulting in a dissimilar embedding representation. Due to the distribution shift between the source and target domains, samples from the same domain are expected to have more concepts in common and, therefore, have more similar representations than samples from different domains. Such assumptions lead to a scenario similar to the one represented in the top left of figure 2. The embeddings of samples from the same domain and class form a well-defined cluster in the space encoded by f_θ . Also, the clusters of samples from the same class, but different domains, are closer together and, ideally, both are distant from all the other clusters.

To summarize, we assume that 1) a good pre-trained model can extract invariant discriminative features, 2) samples from the same class are close in the embedding space, even if they are from different domains, and 3) samples from different classes are distant in the embedding space. Similar

assumptions are proposed by Shen et al. (2022) when studying the generalization of embeddings to out-of-distribution samples.

3.3 THE POTENTIAL ADAPTABILITY SCORE

We introduce the Potential Adaptability Score (**PAS**) as a measure of the distance from a labeled source dataset to an unlabeled target dataset in the embedding space encoded by a pre-trained feature extractor. The **PAS** score is based on the expectation that each target sample is as close as possible to source samples from a single class and significantly distant from source samples from all other classes in the embedding space defined by a pre-trained model f_θ . This means that a target sample is very similar to source samples from one class and has only a few concepts in common with source samples from all other classes, as illustrated in figure 2. The higher the **PAS** value, the stronger the evidence that the pre-trained model can identify invariant discriminative features between the domains and, consequently, the higher the chances that the pre-trained feature extractor f_θ has a good transferability from the source to the target samples.

The samples are normalized to unit length, and the distance between samples is calculated using the cosine distance. We assume that the samples from the class $c \in \mathcal{Y}$ are clustered together. We follow Dhillon & Modha (2001) and compute the centroid of each source class cluster c so they represent the vector that, on average, has the highest cosine similarity to all the samples in the cluster.

$$\mu_c = \frac{\sum_{x_i^S \in S_c^S} f_\theta(x_i^S)}{\|\sum_{x_i^S \in S_c^S} f_\theta(x_i^S)\|}. \quad (1)$$

For each target sample x_i^T , we calculate its cosine distance to the centroid of each source cluster:

$$\text{dist}(f_\theta(x_i^T), \mu_c) = 1 - (f_\theta(x_i^T) \cdot \mu_c). \quad (2)$$

Let $D_i = \{\text{dist}(f_\theta(x_i^T), \mu_1), \dots, \text{dist}(f_\theta(x_i^T), \mu_C)\}$ be the set of distances of the j -th target sample to all the source clusters and $\text{sort}(d_i)$ the sorted version of the set in ascending order. We define $d_{1i} = \text{sort}(D_i)[1]$ and $d_{2i} = \text{sort}(D_i)[2]$ as the shortest and the second shortest of the distances, respectively, as illustrated at the bottom of figure 2.

Finally, the **PAS** score is defined by

$$\text{PAS}(\theta, \mathcal{D}^S, \mathcal{D}^T) = \frac{1}{|\mathcal{D}^T|} \sum_i^{} \frac{d_{2i} - d_{1i}}{d_{2i}}. \quad (3)$$

Given one or more candidate source domains and a set of pre-trained models, the **PAS** score can help to select the options that are more likely to lead to the best accuracy on the target samples. The selection is done by computing the **PAS** score for each trio of target domain, source domain, and pre-trained model. The combination with the highest **PAS** value is chosen. The selection is done before any domain adaptation training. A single-source domain adaptation method can then be trained with the selected source domain and pre-trained feature extractor.

Our **PAS** score is inspired by the Silhouette score, used for assessing the consistency of data clusters Rousseeuw (1987). The Silhouette is a supervised score calculated by $(b - a)/\max\{a, b\}$, where a is the mean intra-cluster distance and b is the mean nearest-cluster distance for each sample. It ranges from -1 to 1 , with higher values indicating strong intra-class cohesion and clear inter-class separation. Note that the Silhouette score is fully supervised and designed for IID samples and its original form is not suitable for the domain adaptation problem. Our **PAS** score is an adaptation to accommodate unlabeled target samples and domain shift. We consider the closest source cluster as the true class for each target sample. This assumption makes a always smaller than b , and restricts our score to the interval $[0, 1]$. The **PAS** score is close to one if the samples from the target domain are similar to the centroid of the source class cluster. However, due to the mismatch between the domains, the target samples exhibit a shift in the feature distribution, making a larger than in the IID scenario. As a result, the values for our score are typically smaller. Alternative design choices are discussed and evaluated in section 4.4.

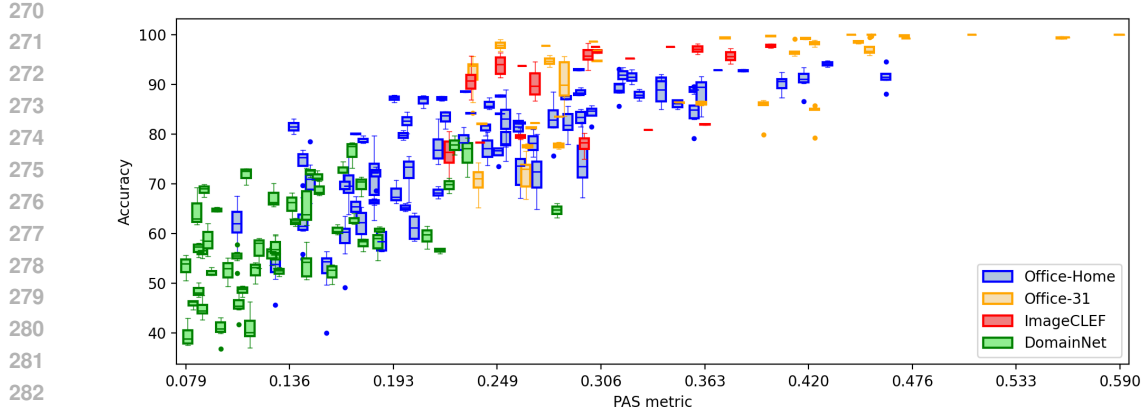


Figure 3: The correlation between the **PAS** score value and the target accuracy after the domain adaptation. Each box summarizes the target accuracy of different domain adaptation methods for a given source-target pair and a pre-trained feature extractor. Higher values for the **PAS** score are strongly correlated with higher target accuracy.

4 EXPERIMENTS

Datasets. We evaluate **PAS** on four of the most popular benchmarks for domain adaptation: **Office-Home** Venkateswara et al. (2017), **Office-31** Saenko et al. (2010), **ImageCLEF**¹, and **DomainNet** Peng et al. (2019). The benchmarks’ statistics are listed in the table 2.

Domain adaptation methods Many domain adaptation methods have been proposed in the literature, but none have consistently outperformed the others in all benchmarks. For this reason, we obtained the published target accuracies of a large variety of state-of-the-art methods. We consider methods based on different paradigms and trained using diverse pre-trained feature extractors. The accuracy values are obtained from the popular open-source *Tllib* library for transfer learning Jiang et al. (2022); Junguang Jiang (2020), Wang et al. (2023), and from the original papers.

Baselines To the best of our knowledge, **PAS** is the first *asymmetric* score proposed for transferability estimation for domain adaptation. We, therefore, compare **PAS** with the symmetric metrics **Maximum Mean Discrepancy (MMD)** Gretton et al. (2012) and **\mathcal{A} -distance** Peng et al. (2019). The MMD distance is computed using a Gaussian kernel. Due to the quadratic nature of MMD, we restrict its computation to a maximum of 10,000 randomly selected samples per domain for the DomainNet benchmark. The **\mathcal{A} -distance** is computed using C-Support Vector Classification. We also report the results for an oracle baseline. The oracle is similar to **PAS**, defined as $\frac{1}{|\mathcal{D}^T|} \sum_i^{|D^T|} \frac{d_{2i} - d_{1i}}{\max\{d_{1i}, d_{2i}\}}$. The d_{1i} distance is the cosine distance to the centroid of the true class of the target sample (not known in real scenarios), and d_{2i} is the distance to the closest cluster’s centroid that is not the true class. In the ideal case where the closest class centroid is the actual class of the sample, the oracle is the same as **PAS**, otherwise, the oracle value is smaller. The oracle validates the existing relationship between the clusters distance and the target accuracy.

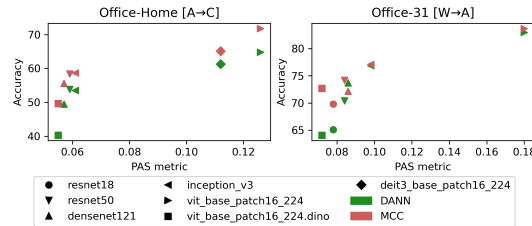


Figure 4: The **PAS** value and target accuracy for the **DANN** and **MCC** methods using different pre-trained feature extractors. The **PAS** score can help to select the feature extractor that leads to higher accuracy. (left) $A \rightarrow C$ adaptation in the *Office-Home* benchmark. (right) $W \rightarrow A$ adaptation in the *Office-31* benchmark.

¹<http://imageclef.org/2014/adaptation>

324

325 Table 1: Average target accuracy of domain adaptation methods and transferability scores for dif-
 326 ferent image classification benchmarks. The highest values are highlighted. Our **PAS** has a high
 327 correlation with the target accuracy and, for each target domain, attributes the highest value for the
 328 source domain that leads to the highest target accuracy in most scenarios. * Oracle baseline that
 329 considers the target labels.

330

331

	Target Source	A			C			P			R			Correlation with acc.		
		C	P	R	A	P	R	A	C	R	A	C	P	Pearson	Spearman	
ResNet-50	Acc. (avg.)	62.0	61.7	72.5	53.5	52.4	58.9	71.0	70.0	82.1	77.2	70.8	78.7	0.77	0.72	
	MMD (neg.)	-0.135	-0.113	-0.052	-0.135	-0.097	-0.125	-0.113	-0.097	-0.033	-0.052	-0.125	-0.033	0.56	0.57	
	\mathcal{A} -distance (neg.)	-1.876	-1.810	-1.333	-1.876	-1.827	-1.814	-1.810	-1.827	-1.424	-1.333	-1.814	-1.424	0.76	0.78	
	PAS (our)	0.107	0.143	0.201	0.128	0.156	0.166	0.182	0.168	0.288	0.217	0.147	0.254	0.81	0.82	
	Oracle*	0.041	0.037	0.093	-0.022	-0.018	-0.022	0.103	0.100	0.218	0.165	0.096	0.195	0.98	0.93	
DeiT-Small	Acc. (avg.)	74.3	71.7	76.0	58.5	61.2	81.7	83.2	86.0	83.3	82.5	84.1	0.56	0.57		
	MMD (neg.)	-0.106	-0.058	-0.024	-0.106	-0.077	-0.102	-0.058	-0.077	-0.026	-0.024	-0.102	-0.026	0.52	0.57	
	\mathcal{A} -distance (neg.)	-1.865	-1.761	-1.26	-1.865	-1.843	-1.796	-1.761	-1.843	-1.37	-1.26	-1.796	-1.37	0.52	0.57	
	PAS (our)	0.143	0.183	0.25	0.175	0.186	0.204	0.261	0.221	0.348	0.295	0.2	0.301	0.67	0.78	
	Oracle*	0.086	0.112	0.18	0.038	0.037	0.047	0.194	0.155	0.291	0.243	0.147	0.246	0.90	0.93	
DeiT-Base	Acc. (avg.)	81.5	78.8	81.1	69.9	65.4	68.0	86.0	87.7	90.6	87.4	87.2	88.5	0.56	0.57	
	MMD (neg.)	-0.099	-0.056	-0.028	-0.099	-0.091	-0.11	-0.056	-0.091	-0.023	-0.028	-0.11	-0.023	0.56	0.57	
	\mathcal{A} -distance (neg.)	-1.832	-1.81	-1.372	-1.832	-1.907	-1.823	-1.81	-1.907	-1.502	-1.372	-1.823	-1.502	0.48	0.51	
	PAS (our)	0.138	0.176	0.243	0.166	0.172	0.194	0.245	0.209	0.339	0.287	0.193	0.295	0.65	0.73	
	Oracle*	0.09	0.112	0.184	0.048	0.049	0.062	0.191	0.158	0.293	0.245	0.154	0.248	0.88	0.88	
ViT-Small	Acc. (avg.)	80.1	79.8	82.2	66.4	65.2	68.2	84.1	84.2	89.0	88.0	87.2	88.5	0.61	0.49	
	MMD (neg.)	-0.116	-0.082	-0.032	-0.116	-0.115	-0.122	-0.082	-0.115	-0.034	-0.032	-0.122	-0.034	0.53	0.59	
	\mathcal{A} -distance (neg.)	-1.885	-1.883	-1.348	-1.885	-1.927	-1.862	-1.883	-1.927	-1.515	-1.348	-1.862	-1.515	0.53	0.59	
	PAS (our)	0.172	0.198	0.262	0.182	0.199	0.217	0.251	0.235	0.357	0.294	0.219	0.316	0.68	0.83	
	Oracle*	0.132	0.147	0.212	0.084	0.102	0.113	0.211	0.195	0.321	0.26	0.189	0.285	0.87	0.92	
ViT-Base	Acc. (avg.)	83.0	82.7	84.5	73.2	72.2	74.4	88.3	88.6	91.4	90.2	89.5	90.8	0.59	0.57	
	MMD (neg.)	-0.101	-0.069	-0.031	-0.101	-0.106	-0.11	-0.069	-0.106	-0.025	-0.031	-0.11	-0.025	0.59	0.57	
	\mathcal{A} -distance (neg.)	-1.85	-1.845	-1.389	-1.85	-1.952	-1.862	-1.885	-1.952	-1.595	-1.389	-1.885	-1.595	0.47	0.51	
	PAS (our)	0.254	0.28	0.357	0.262	0.271	0.296	0.361	0.339	0.462	0.405	0.316	0.417	0.76	0.85	
	Oracle*	0.215	0.233	0.311	0.173	0.188	0.207	0.317	0.295	0.425	0.37	0.286	0.382	0.88	0.92	
Swin-Base	Acc. (avg.)	88.5	87.7	87.9	78.3	77.1	78.2	91.5	91.9	94.2	92.9	93.0	92.8	0.48	0.45	
	MMD (neg.)	-0.081	-0.085	-0.039	-0.081	-0.104	-0.097	-0.085	-0.104	-0.033	-0.039	-0.097	-0.033	0.42	0.37	
	\mathcal{A} -distance (neg.)	-1.853	-1.892	-1.401	-1.853	-1.95	-1.917	-1.892	-1.95	-1.57	-1.401	-1.917	-1.57	0.42	0.37	
	PAS (our)	0.232	0.251	0.327	0.231	0.244	0.269	0.323	0.318	0.43	0.37	0.294	0.384	0.72	0.72	
	Oracle*	0.198	0.214	0.287	0.162	0.177	0.195	0.295	0.282	0.403	0.343	0.27	0.356	0.83	0.81	

349

350

(b) Office-31

	Target Source	D		A		W		D		A		W		Correlation with acc.		
		C	P	A	P	W	D	A	C	P	A	C	W	Pearson	Spearman	
ResNet-50	Acc. (avg.)	71.8	70.6	90.5	100.0	91.9	98.3	71.0	73.7	90.7	90.0	76.0	77.9	0.72	0.72	
	MMD (neg.)	-0.145	-0.165	-0.145	-0.046	-0.165	-0.046	0.71	0.72	-0.022	-0.097	-0.022	-0.022	-0.17	-0.12	
	\mathcal{A} -distance (neg.)	-2.00	-2.00	-2.00	-1.783	-2.00	-1.783	0.72	0.73	-0.807	-1.731	-0.807	-1.731	-0.24	-0.12	
	PAS (our)	0.265	0.239	0.28	0.454	0.238	0.423	0.73	0.66	0.339	0.293	0.239	0.339	0.22	0.49	
	Oracle*	0.192	0.169	0.263	0.445	0.188	0.407	0.80	0.83					0.84	0.71	
DeiT-Small	Acc. (avg.)	77.7	77.6	94.7	99.8	94.65	98.5	77.0	78.7	90.4	90.2	89.5	90.8	0.59	0.57	
	MMD (neg.)	-0.145	-0.165	-0.145	-0.046	-0.165	-0.046	0.71	0.72	-0.022	-0.097	-0.022	-0.022	-0.17	-0.12	
	\mathcal{A} -distance (neg.)	-1.85	-1.845	-1.389	-1.85	-1.952	-1.862	-1.885	-1.952	-1.595	-1.389	-1.885	-1.595	0.47	0.51	
	PAS (our)	0.283	0.266	0.304	0.472	0.278	0.447	0.72	0.73	0.339	0.293	0.239	0.339	0.41	0.52	
	Oracle*	0.2	0.193	0.263	0.465	0.239	0.438	0.80	0.83					0.83	0.83	
DeiT-Base	Acc. (avg.)	81.3	82.0	96.8	100.0	97.9	99.2	77.0	79.7	90.4	90.2	89.5	90.8	0.59	0.57	
	MMD (neg.)	-0.113	-0.134	-0.113	-0.074	-0.134	-0.074	0.54	0.60					0.56	0.57	
	\mathcal{A} -distance (neg.)	-2.00	-2.00	-2.00	-1.969	-2.00	-1.969	0.65	0.60					0.0	0.0	
	PAS (our)	0.283	0.266	0.304	0.472	0.278	0.447	0.72	0.73	0.339	0.293	0.239	0.339	0.41	0.52	
	Oracle*	0.2	0.193	0.263	0.465	0.239	0.438	0.80	0.83					0.83	0.83	
ViT-Small	Acc. (avg.)	83.5	82.2	98.6	100.0	97.7	99.2	77.0	79.7	90.4	90.2	89.5	90.8	0.59	0.57	
	MMD (neg.)	-0.175	-0.197	-0.175	-0.098	-0.197	-0.098	0.56	0.84					-0.17	-0.11	
	\mathcal{A} -distance (neg.)	-2.00	-2.00	-2.00	-2.00	-2.00	-2.00	0.0	0.0					0.0	0.0	
	PAS (our)	0.283	0.27	0.302	0.509	0.276	0.473	0.61	0.94	0.363	0.322	0.263	0.332	0.41	0.52	
	Oracle*	0.23	0.22	0.286	0.506	0.256	0.467	0.69	0.69					0.83	0.83	
ViT-Base	Acc. (avg.)	86.2	86.3	99.7	100.0	99.4	99.5	77.0	79.7	90.4	90.2	89.5	90.8	0.59	0.60	
	MMD (neg.)	-0.168	-0.168	-0.168	-0.086	-0.169	-0.086	0.51	0.60					0.56	0.57	
	\mathcal{A} -distance (neg.)	-2.00	-2.00	-2.00	-2.00	-2.00	-2.00	0.0	0.0					0.0	0.0	
	PAS (our)	0.423	0.395	0.453	0.59	0.412	0.558	0.71	0.83	0.363	0.322	0.263	0.363	0.55	0.54	
	Oracle*	0.373	0.347	0.434	0.589	0.393	0.554	0.79	0.84					0.84	0.84	
Swin-Base	Acc. (avg.)	86.2	86.3	99.7	100.0	99.4	99.5	77.0	79.7	90.4	90.2	89.5	90.8	0.59	0.60	
	MMD (neg.)	-0.168	-0.168	-0.168	-0.086	-0.169	-0.086	0.51	0.60					0.56	0.57	
	\mathcal{A} -distance (neg.)	-2.00	-2.00	-												

378 Table 2: Statistics of the benchmarks used in the experiments.
379

380 Dataset	381 #Samples	382 #Classes	383 Domains
384 Office-Home	385 15,588	386 65	387 A (Art), C (Clipart), P (Product), R (Real-world)
388 Office-31	389 4,110	390 31	391 A (Amazon), D (DSLR), W (Webcam)
392 ImageCLEF	393 1,800	394 12	395 C (Caltech-256), I (ImageNet ILSVRC 2012), P (Pascal VOC 2012)
396 DomainNet	397 569,010	398 345	399 C (Clipart), P (Painting), R (Real), S (Sketch)

385
386 Table 3: Correlation with the average target accuracy after adaptation. Showing Pearson correlation
387 / Spearman’s rank correlation.
388

389	390	391 Office-Home	392 Office-31	393 ImageCLEF	394 DomainNet	395 Total
396 MMD	397 0.55 / 0.51	398 0.45 / 0.53	399 -0.14 / -0.08	400 -0.09 / -0.03	401 0.37 / 0.37	402
403 \mathcal{A} -distance	404 0.32 / 0.17	405 0.26 / 0.35	406 -0.13 / -0.07	407 0.07 / 0.06	408 0.04 / -0.16	409
410 PAS (our)	411 0.76 / 0.81	412 0.63 / 0.78	413 0.44 / 0.60	414 0.53 / 0.56	415 0.83 / 0.88	416
417 Oracle*	418 0.89 / 0.90	419 0.71 / 0.86	420 0.78 / 0.85	421 0.21 / 0.21	422 0.88 / 0.91	423

397
398 4.1 SELECTION OF THE SOURCE DOMAIN

400 The results for the four benchmark datasets are presented in Table 1 (a) - (d). For each source-target
401 pair in the benchmarks, we group the domain adaptation methods using the same pre-trained feature
402 extractor and report their average target accuracy, followed by the baselines and our **PAS** score.
403 We highlight the highest values among the different choices of source domains. We also report
404 the correlation (Pearson and Spearman’s rank correlation) between the average target accuracy and
405 the scores. The detailed results for each individual domain adaptation method are presented in the
406 Supplementary Material A.1.

407 We report in Table 3 the overall correlation for all scenarios of each benchmark (all target domains,
408 source domains and pre-trained models). The results show that the **PAS** score is strongly correlated
409 with target accuracy. We observe an overall Spearman’s rank correlation of **0.88** over all the results.

410 The most important results are reported in Table 4, where we present the correlation for each target
411 domain. This correlation is the most useful for users in real-world scenarios. Given a target domain
412 of interest and many options of source domains and pre-trained models, we show that our **PAS**
413 score has a strong correlation with the final target accuracy. The empirical results indicate that our
414 proposed **PAS** score is effective in selecting the best source domain among many candidates.

415 We summarize our results in Figure 3. Each box in the graph represents the target accuracy of dif-
416 ferent domain adaptation methods using the same pre-trained backbone for a source-target domains
417 pair. We observe that higher **PAS** values are consistently related to high accuracy on the target
418 domain. This indicates that **PAS** may be useful not only for selecting the most appropriate source
419 domain, but also to estimate beforehand the success of the domain adaptation.

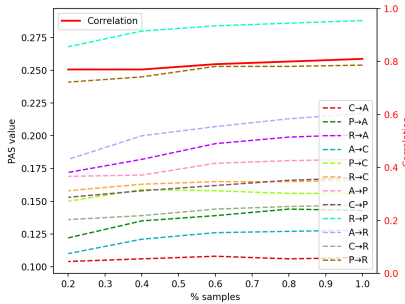
420 The results on the *ImageCLEF* benchmark illustrate the scenarios where the **PAS** score is not ef-
421 fective. This benchmark (especially the *P* domain) contains images with multiple objects. In many
422 cases, the sample is very close to the centroid of one class that is indeed present in the image, but
423 the true label is related to another object in the scene. In these cases, the **PAS** for the sample is

424
425 Table 4: Correlation with the average target accuracy after adaptation for each target domain. Each
426 cell considers the results for a target domain and all available source domains and pre-trained mod-
427 els. Showing Pearson correlation / Spearman’s rank correlation.
428

	Office-Home				Office-31				ImageCLEF				DomainNet			
	A	C	P	R	A	D	W	C	I	P	C	P	R	S		
MMD	0.41 / 0.26	0.28 / 0.21	0.41 / 0.29	0.25 / 0.21	-0.02 / -0.15	0.44 / 0.60	0.45 / 0.36	0.54 / 0.49	-0.03 / -0.22	0.61 / 0.60	-0.56 / -0.42	0.33 / 0.20	0.23 / 0.47	-0.38 / -0.42		
\mathcal{A} -distance	0.12 / -0.13	-0.46 / -0.43	0.15 / -0.09	-0.05 / -0.26	-0.19 / -0.31	0.27 / 0.28	0.14 / 0.07	0.43 / 0.38	0.10 / 0.05	0.64 / 0.60	0.09 / -0.04	0.35 / 0.17	0.27 / 0.30	-0.10 / -0.32		
PAS (our)	0.70 / 0.70	0.81 / 0.78	0.79 / 0.74	0.75 / 0.75	0.65 / 0.81	0.70 / 0.81	0.70 / 0.75	0.82 / 0.76	0.73 / 0.66	0.87 / 0.83	0.71 / 0.67	0.75 / 0.76	0.59 / 0.71	0.48 / 0.35		
Oracle*	0.82 / 0.85	0.91 / 0.90	0.84 / 0.81	0.80 / 0.87	0.74 / 0.88	0.73 / 0.90	0.74 / 0.78	0.81 / 0.76	0.74 / 0.66	0.97 / 0.94	0.36 / 0.50	0.71 / 0.62	0.61 / 0.72	0.28 / 0.33		

432 high, showing a high similarity with one source class, but the final accuracy is low, as the sample is
 433 classified as the wrong class. We show examples in the supplementary material A.2
 434

435 4.2 THE SELECTION OF THE PRE-TRAINED FEATURE EXTRACTOR



449 Figure 5: The **PAS** value varying with
 450 the number of samples for the *Office-Home*. The **PAS** values are quite robust
 451 to varying numbers of samples. Most
 452 importantly, the relative order of **PAS**
 453 values for different source domains
 454 remains unchanged.

455 may be applied for the selection of the pre-trained model.

448
 449 The results in the literature presented in table 1 compare
 450 methods with different backbones and demonstrate
 451 that **PAS** can be applied to select the most suitable pre-
 452 trained feature extractor. However, they do not consider
 453 the impact of different pre-trained feature extractors over the same domain adaptation method. For
 454 analyzing the robustness of **PAS** over different choices
 455 of pre-trained methods, we keep the domain adaptation
 456 method fixed and vary the pre-trained backbone. We se-
 457 lect two of the most challenging domain adaptation sce-
 458 narios: the $A \rightarrow C$ adaptation in the *Office-Home* bench-
 459 mark and $W \rightarrow A$ adaptation in the *Office-31* benchmark.
 460 We show results for two popular domain adaptation meth-
 461 ods: *DANN* Ganin et al. (2016) and *MCC* Jin et al. (2020).
 462 We train each method following the code provided by the
 463 *Tllib* library Jiang et al. (2022); Junguang Jiang (2020)
 464 with the default hyperparameters. The results are shown
 465 in figure 4. Higher **PAS** values are attributed to pre-
 466 trained models that lead to higher target accuracy before
 467 performing domain adaptation, indicating that our score
 468 may be applied for the selection of the pre-trained model.

469 4.3 THE IMPACT OF THE SAMPLE SIZE

470 The time complexity of the **PAS** computation is linear in the number of samples. This can be limiting
 471 for a quick evaluation of larger datasets and scenarios with many candidate source domains.

472 To optimize the computation time, we show that our score can be calculated using only a subset of
 473 the samples. We randomly select a subset of the samples of both source and target domains. The
 474 results are presented in the figure 5. The **PAS** values are quite robust to varying numbers of samples.
 475 Most importantly, the relative order of **PAS** values for different source domains remains unchanged.

476 4.4 DESIGN CHOICES

477 The **PAS** score considers the cosine dis-
 478 tance between each target sample and the
 479 source class centroids. We experimentally
 480 evaluated alternative design choices and
 481 compare the correlation between the score
 482 and the target accuracy. The results are
 483 shown in table 5 and demonstrate how the
 484 overall correlation between the target ac-
 485 curacy and **PAS**, as proposed, is higher.

486 We change **PAS** to consider the Euclidean
 487 distance instead of the cosine distance.
 488 In the domain adaptation setting, the
 489 cosine distance has advantages over using
 490 the Euclidean distance in the original lat-
 491 ent space, as it ignores the magnitude of
 492 representations (e.g., a difference in the illumination in images that reflects on the intensity of the
 493 features detected by the model) and focuses only on the differences in the angles (the difference
 494 between classes). Also, the cosine distance is less affected by the high-dimensionality of the data
 495 (the phenomenon known as *curse of dimensionality* Bellman (1966)).

	Office-Home	Office-31	ImageCLEF	DomainNet	Total
PAS	0.76	0.63	0.44		0.58 0.79
Euclidean distance	0.70	0.69	0.27	0.54	0.68
Average cosine distance	0.66	0.52	0.12	0.48	0.66

477 Table 5: Pearson correlation between the target accuracy and the **PAS** score, which considers the cosine distance to the cluster centroid, and modifications using the Euclidean distance to the centroid and the average cosine distance to the source cluster samples. The maximum correlation value for each benchmark is highlighted. The design choices of **PAS** lead to the higher overall correlation between the score and the target accuracy.

486 We also modify **PAS** to use the average pairwise distance to the source samples instead of the dis-
 487 tance to the source cluster centroid. The pairwise distance is a good summarization of the closeness
 488 of the target sample to the source samples of the class. On the other hand, the distance to the centroid
 489 measures how well the target sample is aligned to the dimensions of greatest alignment between the
 490 samples in the cluster, as the centroid formulation $1/n \sum_{i=1}^{|D^S|} x_i^S$ makes samples pointing in similar
 491 directions add up in that direction.

493 5 CONCLUSION AND FUTURE WORK

495 We present **Potential Adaptability Score (PAS)**, a new score to select, among many candidates, the
 496 source domain or pre-trained model that are likely to lead to the best target accuracy when used for
 497 unsupervised domain adaptation. We evaluate our score on four of the most popular benchmarks for
 498 domain adaptation and show that it has a high correlation with the target accuracy and selects the
 499 best source domain in most cases. We also show that **PAS** can be computed more efficiently with
 500 fewer samples.

501 We suggest two improvements for future work. Although our score could be applied to any classifi-
 502 cation task, we focus on vision problems, specifically the image classification task, which is the most
 503 common task in the domain adaptation literature. Showing its efficacy on other modalities and tasks
 504 demands the availability of a diverse set of benchmarks and specialized domain adaptation methods.
 505 Also, we focus on the single-source domain adaptation problem, where only a single source do-
 506 main is considered during the training. Future works may extend our work to select multiple source
 507 domains, in the setting known as multi-source domain adaptation.

509 ETHICS STATEMENT

511 Although our work does not directly address issues of social harm, we acknowledge that our **PAS**
 512 score is not immune to bias and fairness concerns. If a biased model achieves higher accuracy on the
 513 target data, our framework is likely to select it as the best pre-trained model for domain adaptation.
 514 In our experiments, we mitigate such risks by focusing on pre-trained models and benchmarks that
 515 are widely adopted within the research community.

517 REFERENCES

519 Shadi Alijani, Jamil Fayyad, and Homayoun Najjaran. Vision transformers in domain adaptation
 520 and domain generalization: a study of robustness. *Neural Computing and Applications*, 36(29):
 521 17979–18007, 2024.

522 Yajie Bao, Yang Li, Shao-Lun Huang, Lin Zhang, Lizhong Zheng, Amir Zamir, and Leonidas
 523 Guibas. An information-theoretic approach to transferability in task transfer learning. In *2019*
 524 *IEEE international conference on image processing (ICIP)*, pp. 2309–2313. IEEE, 2019.

525 Richard Bellman. Dynamic programming. *science*, 153(3731):34–37, 1966.

527 Bharath Bhushan Damodaran, Benjamin Kellenberger, Rémi Flamary, Devis Tuia, and Nicolas
 528 Courty. Deepjdot: Deep joint distribution optimal transport for unsupervised domain adaptation.
 529 In *Proceedings of the European conference on computer vision (ECCV)*, pp. 447–463, 2018.

530 Bin Deng and Kui Jia. Universal domain adaptation from foundation models: A baseline study.
 531 *arXiv preprint arXiv:2305.11092*, 2023.

533 Jia Deng, Wei Dong, Richard Socher, Li-Jia Li, Kai Li, and Li Fei-Fei. Imagenet: A large-scale hi-
 534 erarchical image database. In *2009 IEEE conference on computer vision and pattern recognition*,
 535 pp. 248–255. Ieee, 2009.

536 Inderjit S Dhillon and Dharmendra S Modha. Concept decompositions for large sparse text data
 537 using clustering. *Machine learning*, 42(1):143–175, 2001.

538 Linus Ericsson, Da Li, and Timothy Hospedales. Better practices for domain adaptation. In *Inter-
 539 national Conference on Automated Machine Learning*, pp. 4–1. PMLR, 2023.

540 Yaroslav Ganin, Evgeniya Ustinova, Hana Ajakan, Pascal Germain, Hugo Larochelle, François
 541 Laviolette, Mario Marchand, and Victor Lempitsky. Domain-adversarial training of neural net-
 542 works. *The journal of machine learning research*, 17(1):2096–2030, 2016.

543

544 Arthur Gretton, Karsten Borgwardt, Malte Rasch, Bernhard Schölkopf, and Alex Smola. A kernel
 545 method for the two-sample-problem. *Advances in neural information processing systems*, 19,
 546 2006.

547 Arthur Gretton, Karsten M Borgwardt, Malte J Rasch, Bernhard Schölkopf, and Alexander Smola.
 548 A kernel two-sample test. *The journal of machine learning research*, 13(1):723–773, 2012.

549

550 Junguang Jiang, Yang Shu, Jianmin Wang, and Mingsheng Long. Transferability in deep learning:
 551 A survey, 2022.

552

553 Ying Jin, Ximei Wang, Mingsheng Long, and Jianmin Wang. Minimum class confusion for versatile
 554 domain adaptation. In *Computer Vision–ECCV 2020: 16th European Conference, Glasgow, UK,
 555 August 23–28, 2020, Proceedings, Part XXI 16*, pp. 464–480. Springer, 2020.

556

557 Bo Fu Mingsheng Long Junguang Jiang, Baixu Chen. Transfer-learning-library. <https://github.com/thuml/Transfer-Learning-Library>, 2020.

558

559 Donghyun Kim, Kaihong Wang, Stan Sclaroff, and Kate Saenko. A broad study of pre-training for
 560 domain generalization and adaptation. In *European Conference on Computer Vision*, pp. 621–
 561 638. Springer, 2022.

562

563 Ziyue Li, Kan Ren, Xinyang Jiang, Yifei Shen, Haipeng Zhang, and Dongsheng Li. Simple: Special-
 564 ized model-sample matching for domain generalization. In *The Eleventh International Conference
 565 on Learning Representations*, 2023.

566

567 Hong Liu, Jianmin Wang, and Mingsheng Long. Cycle self-training for domain adaptation. *Ad-
 568 vances in Neural Information Processing Systems*, 34:22968–22981, 2021.

569

570 Xiaofeng Liu, Chaehwa Yoo, Fangxu Xing, Hyejin Oh, Georges El Fakhri, Je-Won Kang, Jonghye
 571 Woo, et al. Deep unsupervised domain adaptation: A review of recent advances and perspectives.
APSIPA Transactions on Signal and Information Processing, 11(1), 2022.

572

573 Mingsheng Long, Yue Cao, Jianmin Wang, and Michael Jordan. Learning transferable features with
 574 deep adaptation networks. In *International conference on machine learning*, pp. 97–105. PMLR,
 2015.

575

576 Mingsheng Long, Han Zhu, Jianmin Wang, and Michael I Jordan. Deep transfer learning with joint
 577 adaptation networks. In *International conference on machine learning*, pp. 2208–2217. PMLR,
 2017.

578

579 Mingsheng Long, Zhangjie Cao, Jianmin Wang, and Michael I Jordan. Conditional adversarial
 580 domain adaptation. *Advances in neural information processing systems*, 31, 2018.

581

582 Yiran Luo, Joshua Feinglass, Tejas Gokhale, Kuan-Cheng Lee, Chitta Baral, and Yezhou Yang.
 583 Grounding stylistic domain generalization with quantitative domain shift measures and synthetic
 584 scene images. In *Proceedings of the IEEE/CVF Conference on Computer Vision and Pattern
 585 Recognition*, pp. 7303–7313, 2024.

586

587 Amiel Meiseles and Lior Rokach. Source model selection for deep learning in the time series
 588 domain. *IEEE Access*, 8:6190–6200, 2020.

589

590 Cuong Nguyen, Tal Hassner, Matthias Seeger, and Cedric Archambeau. Leep: A new measure
 591 to evaluate transferability of learned representations. In *International Conference on Machine
 592 Learning*, pp. 7294–7305. PMLR, 2020.

593

594 Michal Pándy, Andrea Agostinelli, Jasper Uijlings, Vittorio Ferrari, and Thomas Mensink. Trans-
 595 ferability estimation using bhattacharyya class separability. In *Proceedings of the IEEE/CVF
 596 Conference on Computer Vision and Pattern Recognition*, pp. 9172–9182, 2022.

594 Xingchao Peng, Ben Usman, Kuniaki Saito, Neela Kaushik, Judy Hoffman, and Kate Saenko.
 595 Syn2real: A new benchmark for synthetic-to-real visual domain adaptation. *arXiv preprint*
 596 *arXiv:1806.09755*, 2018.

597 Xingchao Peng, Qinxun Bai, Xide Xia, Zijun Huang, Kate Saenko, and Bo Wang. Moment matching
 598 for multi-source domain adaptation. In *Proceedings of the IEEE/CVF international conference*
 599 *on computer vision*, pp. 1406–1415, 2019.

601 Chuan-Xian Ren, Yiming Zhai, You-Wei Luo, and Hong Yan. Towards unsupervised domain adap-
 602 tation via domain-transformer. *International Journal of Computer Vision*, 132(12):6163–6183,
 603 2024.

604 Peter J Rousseeuw. Silhouettes: a graphical aid to the interpretation and validation of cluster analy-
 605 sis. *Journal of computational and applied mathematics*, 20:53–65, 1987.

607 Kate Saenko, Brian Kulis, Mario Fritz, and Trevor Darrell. Adapting visual category models to
 608 new domains. In *Computer vision–ECCV 2010: 11th European conference on computer vision,*
 609 *Heraklion, Crete, Greece, September 5-11, 2010, proceedings, part iV 11*, pp. 213–226. Springer,
 610 2010.

612 Kendrick Shen, Robbie M Jones, Ananya Kumar, Sang Michael Xie, Jeff Z HaoChen, Tengyu Ma,
 613 and Percy Liang. Connect, not collapse: Explaining contrastive learning for unsupervised domain
 614 adaptation. In *International conference on machine learning*, pp. 19847–19878. PMLR, 2022.

615 Kihyuk Sohn, David Berthelot, Nicholas Carlini, Zizhao Zhang, Han Zhang, Colin A Raffel,
 616 Ekin Dogus Cubuk, Alexey Kurakin, and Chun-Liang Li. Fixmatch: Simplifying semi-supervised
 617 learning with consistency and confidence. *Advances in neural information processing systems*,
 618 33:596–608, 2020.

620 Baochen Sun and Kate Saenko. Deep coral: Correlation alignment for deep domain adaptation. In
 621 *Computer vision–ECCV 2016 workshops: Amsterdam, the Netherlands, October 8-10 and 15-16,*
 622 *2016, proceedings, part III 14*, pp. 443–450. Springer, 2016.

623 Hui Tang and Kui Jia. A new benchmark: On the utility of synthetic data with blender for bare super-
 624 vised learning and downstream domain adaptation. In *Proceedings of the IEEE/CVF Conference*
 625 *on Computer Vision and Pattern Recognition*, pp. 15954–15964, 2023.

627 Piotr Teterwak, Kuniaki Saito, Theodoros Tsilgkardis, Kate Saenko, and Bryan A Plummer.
 628 Erm++: An improved baseline for domain generalization. *arXiv preprint arXiv:2304.01973*,
 629 2023.

631 Anh T Tran, Cuong V Nguyen, and Tal Hassner. Transferability and hardness of supervised classi-
 632 fication tasks. In *Proceedings of the IEEE/CVF international conference on computer vision*, pp.
 633 1395–1405, 2019.

634 Eric Tzeng, Judy Hoffman, Ning Zhang, Kate Saenko, and Trevor Darrell. Deep domain confusion:
 635 Maximizing for domain invariance. *arXiv preprint arXiv:1412.3474*, 2014.

637 Eric Tzeng, Judy Hoffman, Kate Saenko, and Trevor Darrell. Adversarial discriminative domain
 638 adaptation. In *Proceedings of the IEEE conference on computer vision and pattern recognition*,
 639 pp. 7167–7176, 2017.

640 SS Vallender. Calculation of the wasserstein distance between probability distributions on the line.
 641 *Theory of Probability & Its Applications*, 18(4):784–786, 1974.

643 Hemanth Venkateswara, Jose Eusebio, Shayok Chakraborty, and Sethuraman Panchanathan. Deep
 644 hashing network for unsupervised domain adaptation. In *Proceedings of the IEEE Conference on*
 645 *Computer Vision and Pattern Recognition*, pp. 5018–5027, 2017.

647 Qian Wang, Fanlin Meng, and Toby P Breckon. Data augmentation with norm-ae and selective
 648 pseudo-labelling for unsupervised domain adaptation. *Neural Networks*, 161:614–625, 2023.

648	Kaichao You, Xime Wang, Mingsheng Long, and Michael Jordan. Towards accurate model selec-														
649	tion in deep unsupervised domain adaptation. In <i>International Conference on Machine Learning</i> , pp. 7124–7133. PMLR, 2019.														
650															
651															
652	Kaichao You, Yong Liu, Jianmin Wang, and Mingsheng Long. Logme: Practical assessment of														
653	pre-trained models for transfer learning. In <i>International Conference on Machine Learning</i> , pp. 12133–12143. PMLR, 2021.														
654															
655															
656	Wen Zhang, Lingfei Deng, Lei Zhang, and Dongrui Wu. A survey on negative transfer. <i>IEEE/CAA</i>														
657	<i>Journal of Automatica Sinica</i> , 10(2):305–329, 2022.														
658															
659	Jinjing Zhu, Haotian Bai, and Lin Wang. Patch-mix transformer for unsupervised domain adapta-														
660	tion: A game perspective. In <i>Proceedings of the IEEE/CVF conference on computer vision and</i>														
661	<i>pattern recognition</i> , pp. 3561–3571, 2023.														
662	Yang Zou, Zhiding Yu, Xiaofeng Liu, BVK Kumar, and Jinsong Wang. Confidence regularized														
663	self-training. In <i>Proceedings of the IEEE/CVF International Conference on Computer Vision</i> , pp. 5982–5991, 2019.														
664															
665															
666															
667	A SUPPLEMENTARY MATERIAL														
668															
669															
670	A.1 RESULTS														
671	The tables 6, 7, 8, and 9 show the extended results of table 1. The accuracy for each method is listed,														
672	as well as its accuracy correlation with the scores.														
673															
674	Table 6: Target accuracy of domain adaptation methods and transferability scores for the <i>Office-</i>														
675	<i>Home</i> dataset. The highest values are highlighted. * Oracle baseline that considers the target labels.														
676															
677															
678															
679															
680															
681															
682															
683															
684															
685															
686															
687															
688															
689															
690															
691															
692															
693															
694															
695															
696															
697															
698															
699															
700															
701															
	Target Source	C	A P	R	C	P	R	A	P C	R	A C	R P	Correlation with PAS Pearson	Spearman	
ResNet-50	DAN	57.7	54.9	66.2	45.6	40.0	49.1	67.7	63.8	77.9	73.9	66.0	74.5	0.74	0.81
	DANN	55.8	55.8	71.1	53.8	55.1	60.7	62.6	67.3	81.1	74.0	67.3	77.9	0.91	0.85
	ADDA	59.7	61.4	71.1	52.6	52.5	58.6	62.9	68.0	80.2	74.0	68.8	77.6	0.84	0.80
	JAN	60.6	60.5	71.0	50.8	49.6	55.9	71.9	68.3	80.5	76.5	68.7	76.9	0.78	0.81
	CDAN	62.0	62.4	75.5	55.2	54.3	61.0	72.4	69.7	83.8	77.6	70.9	80.5	0.85	0.83
	MCD	63.7	61.5	74.5	51.7	52.8	58.4	72.2	69.5	81.8	78.2	70.8	78.0	0.78	0.83
	BSP	61.0	60.9	73.4	54.7	55.2	60.3	67.7	69.4	81.2	76.2	70.9	80.2	0.85	0.80
	AFN	65.0	65.0	72.3	53.2	51.4	57.8	72.7	71.3	82.4	76.8	72.3	77.9	0.73	0.78
	MDD	63.5	62.5	73.5	56.2	54.8	60.9	75.4	72.1	84.5	79.6	73.8	79.9	0.80	0.78
	MCC	67.5	66.6	74.4	58.4	54.8	61.4	79.6	77.0	85.6	83.0	78.5	81.8	0.70	0.76
	FixMatch	65.3	67.2	74.9	56.4	56.4	63.5	76.4	73.8	84.3	79.9	71.2	80.6	0.81	0.87
	Avg.	62.0	61.7	72.5	53.5	52.4	58.9	71.0	70.0	82.1	77.2	70.8	78.7	0.81	0.82
	PAS (our)	0.107	0.143	0.201	0.128	0.156	0.166	0.182	0.168	0.288	0.217	0.147	0.254		
DeiT-Small	TRANS-DA	69.7	68.6	73.5	57.7	56.3	58.5	80.8	83	85	81.5	80.1	81.5	0.69	0.79
	WinTR	76.8	73.4	77.2	65.3	60	63.1	84.1	84.5	86.8	85	84.4	85.7	0.64	0.78
	DOT	74.9	72.4	76.4	63.7	61	64.1	82.2	84.3	86.7	84.3	83	84.8	0.68	0.79
	CDTrans	75.6	72.5	77	60.6	56.7	59.1	79.5	81	85.5	82.4	82.3	84.4	0.63	0.76
	Avg.	74.3	71.7	76.0	61.8	58.5	61.2	81.7	83.2	86	83.3	82.5	84.1	0.67	0.78
	PAS (our)	0.143	0.183	0.25	0.175	0.186	0.204	0.261	0.221	0.348	0.295	0.2	0.301		
DeiT-Base	DOT	80	78.2	79.7	69	65.4	67.3	85.6	85.2	89.3	87	86.4	87.9	0.66	0.75
	CDTrans	81.5	79.6	82	68.8	63.3	66	85	87.1	90.6	86.9	87.3	88.2	0.62	0.73
	PMTrans	83	78.5	81.7	71.8	67.4	70.7	87.3	87.7	92	88.3	87.8	89.3	0.67	0.73
	Avg.	81.5	78.8	81.1	69.9	65.4	68.0	86.0	86.7	90.6	87.4	87.2	88.5	0.65	0.73
ViT-Small	SSRT	79.9	80.7	82	67	66	69.4	84.2	84.3	89.9	88.3	87.6	88.3	0.69	0.84
	SAMB	80.2	78.8	82.4	65.7	64.4	67	84	84.1	88	87.7	86.7	88.6	0.67	0.82
	Avg.	80.1	79.8	82.2	66.4	65.2	68.2	84.1	84.2	89.0	88.0	87.2	88.5	0.68	0.83
	PAS (our)	0.172	0.198	0.262	0.182	0.199	0.217	0.251	0.235	0.357	0.294	0.219	0.316		
ViT-Base	SAMB	80.8	81.6	84.1	68.7	68.7	70.9	85	86	91.1	88.9	88.3	90.2	0.77	0.88
	DoT	81.8	81.2	82.9	72.9	70.6	72.2	89.8	89.6	90.8	90.3	90.1	92.4	0.75	0.84
	TVT	77.4	75.6	79.1	67.1	64.9	67.2	83.5	85	88	87.3	85.6	86.6	0.78	0.85
	SSRT	85.1	85	85.7	75.2	74.2	78.6	89	88.3	91.8	91.1	90	91.3	0.76	0.87
	BCAT	84.2	84.1	85.7	74.2	74.5	74.8	90.6	90.9	92.2	90.9	90.7	90.8	0.74	0.83
	PMTrans	88.9	88.5	89.5	81.2	80	82.4	91.6	91.6	94.5	92.4	93	93.4	0.74	0.84
	Avg.	83.0	82.7	84.5	73.2	72.2	74.4	88.3	88.6	91.4	90.2	89.5	90.8	0.76	0.85
	PAS (our)	0.254	0.28	0.357	0.262	0.271	0.296	0.361	0.339	0.462	0.405	0.316	0.417		
Swin-Base	PMTrans	88.4	87.9	89	81.3	80.4	80.9	92.9	93.4	94.8	92.8	93.2	93	0.75	0.72
	BCAT	88.6	87.4	86.7	75.3	73.7	75.4	90	90.3	93.5	92.9	92.7	92.5	0.68	0.74
	Avg.	88.5	87.7	87.9	78.3	77.1	78.2	91.5	91.9	94.2	92.9	93.0	92.8	0.72	0.72
	PAS (our)	0.232	0.251	0.327	0.231	0.244	0.269	0.323	0.318	0.43	0.37	0.294	0.384		

702 Table 7: Target accuracy of domain adaptation methods and transferability scores for the ***Office-31***
 703 dataset. The highest values are highlighted. * Oracle baseline that considers the target labels.

	Target Source	A		D		W		Correlation with PAS	
		D	W	A	W	A	D	Pearson	Spearman
ResNet-50	DANN	73.3	70.4	83.6	100.0	91.4	97.9	0.78	0.66
	ADDA	69.6	72.5	90.0	99.7	94.6	97.5	0.67	0.60
	BSP	74.1	73.8	88.2	100.0	92.7	97.9	0.75	0.66
	DAN	66.9	65.2	87.3	100.0	84.2	98.4	0.83	0.83
	JAN	69.2	71.0	89.4	100.0	93.7	98.4	0.70	0.60
	CDAN	73.4	70.4	89.9	100.0	93.8	98.5	0.71	0.66
	MCD	68.3	67.6	87.3	100.0	90.4	98.5	0.76	0.66
	AFN	72.9	71.1	94.4	100.0	94.0	98.9	0.67	0.83
	MDD	76.6	72.2	94.4	100.0	95.6	98.6	0.65	0.66
	MCC	75.5	74.2	95.6	99.8	94.1	98.4	0.66	0.83
	FixMatch	70.0	68.1	95.4	100.0	86.4	98.2	0.75	0.83
	Avg. PAS (our)	71.1 0.265	70.0 0.239	89.6 0.286	99.9 0.454	90.6 0.236	98.1 0.423	0.73	0.66
DeiT-Small	TRANS-DA	77	77.1	94.8	100	95.8	98.8	0.69	0.71
	CDTrans	78.4	78	94.6	99.6	93.5	98.2	0.74	0.94
	Avg. PAS (our)	77.7 0.283	77.6 0.266	94.7 0.304	99.8 0.472	94.65 0.278	98.5 0.447	0.72	0.94
DeiT-Base	CDTrans	81.1	81.9	97	100	96.7	99	0.69	0.83
	PMTrans	81.4	82.1	96.5	100	99	99.4	0.64	0.71
	Avg. PAS (our)	81.3 0.268	82.0 0.241	96.8 0.304	100.0 0.443	97.9 0.251	99.2 0.418	0.66	0.71
	ViT-Small	SSRT	83.5	82.2	98.6	100	97.7	99.2	0.61
ViT-Base	PAS (our)	0.283	0.27	0.302	0.509	0.276	0.473		
	DoT	85.1	86.8	96.7	100	96.6	99.4	0.74	0.83
	TVT	84.9	86.1	96.4	100	96.4	99.4	0.75	0.75
	SSRT	79.2	79.9	95.8	100	95.7	99.2	0.72	0.83
	BCAT	84.9	85.8	97.5	100	96.1	99.1	0.73	0.83
	PMTrans	85.7	86.3	99.4	100	99.1	99.6	0.62	0.83
	Avg. PAS (our)	84.0 0.423	85.0 0.395	97.2 0.453	100.0 0.59	96.8 0.412	99.3 0.558	0.71	0.83
Swin-Base	PMTrans	86.7	86.5	99.8	100	99.5	99.4	0.61	0.83
	BCAT	85.7	86.1	99.6	100	99.2	99.5	0.63	0.89
	Avg. PAS (our)	86.2 0.361	86.3 0.349	99.7 0.399	100 0.589	99.4 0.374	99.5 0.56	0.62	0.89

A.2 EXAMPLES OF SAMPLES IN THE *ImageCLEF* BENCHMARK

740 We present some examples of when the **PAS** score fails to predict the target accuracy. The figure 6
 741 shows examples of misclassified images from the **P** (*Pascal VOC 2012*) domain of the *ImageCLEF*
 742 benchmark. Many images contain more than one object. The sample may be very similar to a class
 743 present in the image. However, the true class refers to another object also contained in the image. In
 744 such cases, the **PAS** value is high, but the accuracy is low.

756
 757
 758
 759
Table 8: Target accuracy of domain adaptation methods and transferability scores for the ***Image-CLEF*** dataset. The highest values are highlighted. * Oracle baseline that considers the target labels.
 760
 761

	Target Source	C		I		P		Correlation with PAS	
		I	P	C	P	C	I	Pearson	Spearman
ResNet-50	RTN	95.3	92.2	86.9	86.8	72.7	75.6	0.29	0.49
	MADA	96.0	92.2	88.8	87.9	75.2	75.0	0.20	0.26
	iCAN	94.7	92	89.9	89.7	78.5	79.5	0.23	0.49
	CDAN-E	97.7	94.3	91.3	90.7	74.2	77.7	0.27	0.49
	SymNets	97.0	96.4	93.4	93.6	78.7	80.2	0.17	0.60
	MEDA	95.7	95.5	92.2	92.5	78.5	79.7	0.16	0.60
	SPL	96.7	96.3	95.7	94.5	80.5	78.3	0.02	0.26
	DS-c	92.8	91.3	87.3	86.7	70.4	78.7	0.39	0.49
	CAN	95.5	95.2	91.6	91.8	76.4	78.5	0.19	0.60
	JAN	94.7	91.7	89.5	88.0	74.2	76.8	0.24	0.49
	CDAN	98.3	94	90.7	88.3	76.7	77.2	0.22	0.49
	Avg. PAS (our)	95.9 0.299	93.7 0.251	90.7 0.235	90.0 0.27	76.0 0.223	77.9 0.297	0.22	0.49
DeiT-small	TRANS-DA	97.5	97.5	93.7	95.2	78.3	80.8	0.41	0.52
	PAS (our)	0.344	0.303	0.263	0.322	0.24	0.332		
ViT-Base	VT-ADA	97.3	96.0	96.2	94.1	78.9	81.8	0.55	0.49
	CSTrans	98.2	98.2	97.0	97.2	80.0	82.0	0.54	0.62
	Avg. PAS (our)	97.8 0.399	97.1 0.359	96.6 0.304	95.7 0.377	79.5 0.262	81.9 0.363	0.55	0.54

782
 783
 784
 785
 786
 787
Table 9: Target accuracy of domain adaptation methods and transferability scores for the ***DomainNet*** dataset. The highest values are highlighted. * Oracle baseline that considers the target labels.
 788
 789
 790

	Target Source	C			P			R			S			Correlation with PAS	
		P	R	S	C	R	S	C	P	S	C	P	R	Pearson	Spearman
ResNet-50	DAN	45.9	50.8	56.1	38.8	49.8	45.9	55.2	59.0	55.5	43.9	40.8	38.9	0.54	0.49
	DANN	41.7	50.7	55.0	37.9	50.8	45.0	54.3	55.6	54.5	44.4	36.8	40.1	0.53	0.46
	JAN	47.2	54.2	56.6	40.5	52.6	46.2	56.7	59.9	55.5	45.1	43.0	41.9	0.63	0.58
	CDAN	45.1	55.6	57.2	40.4	53.6	46.4	56.8	58.4	55.7	46.1	40.5	43.0	0.60	0.50
	MCD	44.6	52.0	55.5	37.5	51.5	44.6	52.9	54.5	52.0	44.0	41.6	39.7	0.57	0.47
	MDD	48.6	58.3	58.7	42.9	53.7	46.5	59.5	59.4	57.7	47.5	42.6	46.2	0.60	0.59
	MCC	45.4	54.4	58.1	37.7	53.1	46.3	55.7	59.8	56.2	42.6	39.9	37.0	0.57	0.43
	Avg. PAS (our)	45.5 0.108	53.7 0.145	56.7 0.088	39.4 0.08	52.2 0.159	45.8 0.083	55.9 0.128	58.1 0.184	55.3 0.107	44.8 0.088	40.7 0.098	41.0 0.114	0.58	0.53
	WinTR	53.2	70.5	51.6	62.0	71.3	50.1	63.1	55.9	48.8	65.3	54.1	70.1	0.32	0.54
	DOT	51.3	67.6	51.7	58.5	70.4	47.2	62.3	57	49.4	64.6	49.9	65.4	0.42	0.52
	CDTRANS	52.5	68.3	53.2	55.4	67.4	48	61.5	56.8	47.2	64.3	53.2	66.2	0.41	0.55
	Avg. PAS (our)	52.3 0.13	68.8 0.152	52.2 0.093	58.6 0.091	69.7 0.175	48.4 0.086	62.3 0.139	56.6 0.11	48.5 0.096	64.7 0.117	52.4 0.127	67.2 0.127	0.39	0.57
DeiT-Small	DOT	53.6	71.2	55.2	61.8	72.2	50.5	62.9	56.9	49.3	67.3	52.9	69.8	0.27	0.45
	CDTRANS	57.2	72.6	58.1	62.9	72.1	53.9	66.2	61.5	52.9	69.0	59.0	72.5	0.33	0.43
	WINTR	56.3	72.8	57.3	69.2	74.4	55.6	68.2	59.8	55.1	69.9	58.1	73.1	0.20	0.39
	Avg. PAS (our)	55.7 0.126	72.2 0.147	56.9 0.086	64.6 0.085	72.9 0.165	53.3 0.079	65.8 0.137	59.4 0.102	52.4 0.089	68.7 0.119	56.7 0.112	71.8 0.112	0.26	0.44
DeiT-Base	SAMB	60.5	77.8	61.8	63.8	77.1	56.8	68	64.7	58.4	71.1	64	77.5	0.38	0.43
	DoT	61.3	79.6	60.4	73.2	79.2	59.7	71.1	63.2	56.4	72.6	61.9	78.3	0.24	0.31
	SSRT	60.2	75.8	59.8	61.7	71.4	55.2	69.9	66.0	58.9	70.6	62.2	73.2	0.50	0.46
	Avg. PAS (our)	60.7 0.185	77.7 0.226	60.7 0.162	66.2 0.145	75.9 0.233	57.2 0.128	69.7 0.282	64.6 0.176	57.9 0.151	71.4 0.171	62.7 0.17	76.3 0.17	0.37	0.35
ViT-Base	SAMB	60.5	77.8	61.8	63.8	77.1	56.8	68	64.7	58.4	71.1	64	77.5	0.38	0.43
	DoT	61.3	79.6	60.4	73.2	79.2	59.7	71.1	63.2	56.4	72.6	61.9	78.3	0.24	0.31

810
811
812
813
814
815
816
817
818
819
820
821
822
823
824
825
826
827
828



(a) Predicted: Car |True: Bottle



(b) Predicted: Horse |True: Person



(c) Predicted: Motorcycle |True: Car



(d) Predicted: Plane |True: Bus



(e) Predicted: Person |True: Bottle



(f) Predicted: Dog |True: Bird



(g) Predicted: Bike |True: Bus



(h) Predicted: Car |True: Person



(i) Predicted: Motorcycle |True: Person

851
852
853
854
855
856
857
858
859
860
861
862
863

Figure 6: Examples of images misclassified by the domain adaptation method *DANN* in the dataset *P* (*Pascal VOC 2012*) of the *ImageCLEF* benchmark